Phase relations of phlogopite with and without enstatite up to 8 GPa : implication to potassic magmatism and mantle metasomatism

Kiminori Sato, Tomoo Katsura and Eiji Ito
Institute for Study of the Earth's Interior, Okayama University,
Misasa, Tottori 682-02, Japan

Submitted to Earth and Planetary Science Letters, 1996

Abstract
Stability relations of phlogopite and phlogopite+enstatite systems without additional water have been experimentally determined at pressures of 4 - 8 GPa and at temperatures of 1200 - 1500˚C by using a uniaxial split-sphere apparatus. The phlogopite gradually dissociates into pyrope and Al_2O_3-deficient phlogopite at pressures above 5 GPa. The Al_2O_3 content in the phlogopite decreases from 14.4 wt% at 6 GPa to 12.9 wt% at 8 GPa and concurrently the mode of pyrope increases from <5 modal% at 5.GPa to 20 - 30 % at 8 GPa, in the phlogopite system. Thus increase in pressure enhances two cation substitutions, Al+Al=Mg+Si and Mg+2Al= []+2Si, in the phlogopite structure. The solidi of the phlogopite and phlogopite+enstatite systems reach maximum temperatures of 1350˚C and 1300˚C, respectively, at about 5 GPa. Pyrope is a residual phase under hypersolidus conditions in both the systems above 5 GPa.

The stabilities of phlogopite determined in the present study indicate that phlogopite can be stable in garnet harzburgite in the subcratonic lithosphere down to 210 km depth. The observed decomposition of the phlogopite into an assemblage of garnet and fluid or hydrous silicate melt suggests that phlogopite can be secondarily formed by a reaction of garnet and upwelling metasomatic agents near the base of continental lithosphere.

1. Introduction

It has been recognized that the stability of phlogopite and reaction of phlogopite with K_2O bearing fluid or hydrous silicate melt play important roles in the mantle processes as follows; (1) fluid that is released by break-down of phlogopite lowers the solidus temperature of peridotite and causes magma generation [1], (2) fluid or hydrous silicate melt originated from deeper part of the mantle metasomatizes peridotite and often forms secondarily phlogopite [2,3], and (3) ultrapotassic magma would be produced by partial melting of phlogopite-bearing peridotites formed by the process (2) and thus could be a source of ultrapotassic magma, such as lamproites [4,5]. With regard to the process (2), phlogopite is often found in mantle xenoliths in various tectonic settings [3,6,7,8]. The phlogopite-involving reactions described above are directory related to the pressure-temperature stability limit of phlogopite. Therefore, the determination of stability of phlogopite under the wide range of mantle conditions is of essentially importance to understand the distribution of phlogopite, melting processes and metasomatic phenomena in the upper mantle.

Many workers experimentally investigated the stability of phlogopite under upper mantle conditions [9, 10, 11, 12, 13, 14, 15, 16]. For example, Sudo and Tastumi [1] has reported that phlogopite reacts with clinopyroxene and enstatite to produce K-amphibole ($K_2CaMg_5Si_8O_{22}(OH)_2$), garnet and forsterite at pressures of 6 - 7 GPa in subsolidus condition, suggesting that the high pressure stability of phlogopite in lherzolite is limited by a univariant reaction:

2phlogopite +diopside +2enstatite =K-amphibole +2garnet +2forsterite +fluid (1)

However, phase relations of phlogopite and phlogopite+enstatite systems above 4 GPa have been still remained unclear. Without detailed information of melting relation of phlogopite, the following processes and whereabouts in the mantle these processes take place cannot be discussed properly.

First, phlogopite is often observed in garnet harzburgite xenoliths in kimberlites and is considered to be formed secondarily by the reaction of metasomatic agents such as hydrous silicate melt or fluid and peridotites [2,3,7]. Secondly, composition of liquid generated by low degree of partial melting of phlogopite-bearing rocks are indispensable to understand the formation of ultrapotassic magmas. Third, concerning with the stability of phlogopite, the phase relations of phlogopite +enstatite are required to discuss how phlogopite decomposes or forms in Ca-rich pyroxene-free peridotites or phlogopite-pyroxenites which may be presented in wedge mantle along subducting slab [17,18].

In the present study, the melting and subsolidus phase relations are experimentally investigated on two systems, phlogopite and phlogopite + enstatite, without additional H_2O at pressures of 4 - 8 GPa and at temperatures of 1200 - 1500˚C. Based on these results, stability and secondary formation of phlogopite in the subcratonic mantle are discussed together with lamproite petrogenesis.

2. Experimental and analytical procedure

2.1. Starting materials

Starting materials of phlogopite was natural specimen from Posu mine in Korean peninsula and its chemical composition is shown in Table 1. Enstatite was crystallized at 1500˚C for 48 hours from $MgSiO_3$ glass. Examinations of two phases by electron microprobe analysis and powder X-ray diffractmetry confirmed that both were single phases. These crystalline phases were ground and then dried at 110˚C for more than 24 hours. A single phase of phlogopite and an even weight mixture of phlogopite and enstatite were used as starting materials for the high-pressure and high-temperature experiments. No water was added to the starting materials.

2.2. High-pressure experiments

High-pressure and high-temperature experiments were performed by utilizing a uniaxial split-sphere apparatus [19]. Tungsten carbide cubes of 11 mm truncation were used with a semi-sintered magnesia octahedron of 18 mm edge length as a pressure medium (11-18 system). Sample pressure was calibrated against the oil pressure of the hydraulic press. Pressure calibration curve for the 11 -18 system was constructed by detecting phase the olivine - spinel transition in Fe_2SiO_4 [20] and the olivine - modified spinel transition and the modified spinel - spinel transitions in Co_2SiO_4 [21] at 1300˚.

Cell assembly is schematically shown in Fig. 1. Heating material was graphite with a straight cylindrical shape. A cylindrical sleeve of ZrO_2 was placed outside the graphite heater as a thermal insulator. The temperature was monitored using a W97%Re3%-W75%Re25% thermocouple with a diameter of 0.2 mm, without any correction for the pressure effect on e.m.f. Sample was charged in a sealed Pt capsule of 1.2 or 1.5mm outside diameter, 0.8 or 1.0 mm inside diameter and of 1 - 2 mm length. Temperature distribution in the sample container was measured by simultaneous measurements of temperatures at the hot and the cold ends of the sample container. The temperature difference between both ends was about 50˚C at 1300˚C.

Pressure was applied first and then the sample was heated to a desired temperature. Experimental temperature and pressure were controlled within $\pm$10˚C and $\pm$0.05 GPa of the nominal values, respectively. After kept for a desired duration, the sample was quenched by shutting off the electric power under the working pressure. Temperature went down below 200˚C within a second. The recovered sample was mounted in epoxy resin and made a polished section parallel to the longitudinal direction of the cylindrical heater.

Run durations were 60-120 and 30-90 minutes at temperatures below and above 1300˚C, respectively (Table 2). The attainment of equilibrium was tested by conducting two run durations of 1 and 10 hours on the phlogopite+enstatite system at 6 GPa and 1300oC. The mineral assemblage and chemical composition of 1 hour duration were found to be identical to those of 10 hours duration (Table 3). Thus it was concluded that equilibrium was attained in 1 hour running duration at temperatures above 1300˚C.

2.3. Analyses

Phases present were identified by means of electron microprobe analysis and micro-focused X-ray

diffractmetry. Chemical compositions of the phases were analyzed by using JEOL JXA-8800 electron probe microanalyzer, operated at 15 Kev accelerating voltage. The beam current and diameter were $2X10^{-8}$A and 1 μm, respectively.

A criterion for occurrence of melting was the existence of quench crystal of phlogopite which exhibits needle texture (Fig. 2a,b). When the quench phlogopite coexisted with solid phlogopite in the experimental charge, the former has lower Al_2O_3 content than the latter. Therefore, the Al_2O_3 content of phlogopite was also a good indicator to judge the occurrence of partial melting.

3. Results

3.1. Stability relations of phlogopite and phlogopite+enstatite systems

Table 2 summarizes the experimental results on the systems of phlogopite and phlogopite + enstatite. Figs. 3a and b show phase relations of the phlogopite and the phlogopite+enstatite systems, respectively.

Phlogopite: Up to 4.5 GPa, phlogopite is stable under subsolidus conditions, and incongruently melts into liquid+forsterite. Above 4.5 GPa, pyrope is present under both the subsolidus and hypersolidus conditions. Under subsolidus conditions of 5 - 8 GPa, the starting phlogopite dissociates into an assemblage of Al_2O_3-deficient phlogopite, pyrope and fluid. The amount of pyrope increases with increasing pressure; less than 5 modal % at 5 GPa to 20-30 modal % at 8 GPa. Water drops were actually observed in the run products under the subsolidus conditions, indicating the presence of fluid in the conditions. An assemblage of phlogopite +pyrope melts to forsterite+pyrope+liquid at pressures between 5 and 8 GPa. However, forsterite disappears at temperatures 50 - 100˚C higher than the solidus. The assemblage starts to melt at 1350˚C and 5 GPa, and at 1300˚C and 8 GPa, respectively. Thus solidus curve has a negative dT/dP slope above 5 GPa. It is also noted that $MgAl_2O_4$ spinel coexists with pyrope and forsterite in the limited hypersolidus condition around 5 GPa and 1400˚C (Fig. 3a).

Phlogopite + enstatite: Main features of the phase relations in this system are similar to those of the phlogopite system. For example, pyrope occurs both in the subsolidus and hypersolidus conditions above 5 GPa, and the solidus curve has a negative dT/dP slope above 6 GPa. The solidus curve in this system is about 50˚C lower than that of the phlogopite system at pressures of 4 - 6 GPa, but both are very close at 8 GPa. Coexisting phases with melt just above the solidus are as followings; enstatite, forsterite and phlogopite at 4 GPa, enstatite, forsterite, pyrope and phlogopite at pressure of 5 - 7 GPa, and enstatite, pyrope, and phlogopite above 7 GPa. Coexistence of solid and quench phlogopites was observed in the four runs conducted at 1350˚C and pressures of 4 GPa, 5 GPa and 6 GPa, and in that at 8 GPa and 1300˚C (Fig. 3b), indicating that partial melting of phlogopite occurs in this system just above the solidus conditions. The partial melting of phlogopite in the system of phlogopite+enstatite was confirmed at pressures of 1 - 2.5 GPa, and the temperature range in which melt and phlogopite coexist was reported to be 30-40˚C [11]. The melting interval of phlogopite was found to be certainly less than 100˚C as shown in Fig. 3. However, more specification was impossible, because the temperature variation in the sample was about 50˚C in this study. Thus the melting interval is assumed to be about 40˚C by extrapolation of those at the lower pressures [11] (Fig. 3b). An occurrence of very small amount of forsterite at 5 GPa and 1300˚C, which is marked in the field of enstatite+phlogopite +pyrope +fluid, is due to the thermal gradient through the sample and the running condition should have been very close to the solidus.

3.2. Variation in the composition of phlogopite under subsolidus conditions

Chemical compositions of phlogopite are shown in Table 3. Figs. 4a and b show negative correlation between Al+Al and Mg+Si and that between Mg+2Al and V (vacancy) +2Si in the phlogopites, respectively. The change in phlogopite composition due to the cation substitutions are shown in Fig. 5. Number of vacancy was calculated by subtracting the cation sum of Si, Al, Mg, Fe, Ti and Mn in the phlogopite (represented as #1 in Table 3) from the total number of tetrahedral and octahedral sites in the phlogopite structure. With increasing pressure, the cation numbers of Si and Mg of phlogopite in both systems increase, while that of Al decreases. Therefore, two substitutions, Al+Al -> Mg+Si and Mg+2Al -> []+2Si control the change in composition of phlogopite with pressure. In the phlogopite system, these compositional changes in phlogopite are corresponding to the exsolution of

pyrope, because Mg:Al:Si ratio is 3:2:3 in pyrope and 3:1:3 in phlogopite. Namely, the exsolution of pyrope reduces the relative abundance of Al to Mg and Si in phlogopite. In the phlogopite+enstatite system, the degree of deficiency of Al_2O_3 component in phlogopite is higher than those of the phlogopite system at the same pressure (Fig. 5). This would be responsible to the larger amount of pyrope crystallization in the phlogopite +enstatite system. In the former system, crystallization of pyrope is prompted by the presence of enstatite.

The solidus of the enstatite+phlogopite system between 5 and 6 GPa is univariant curve on which 6 phases exist, provided that 5 components (Al_2O_3, SiO_2, MgO, K_2O and H_2O) comprise the system. This means that K_2O and H_2O behave as independent components in the system. This is consistent with the observation that number of K in phlogopite formula increases at 1300˚C with elevating pressure (Table 2).

3.3. Chemical composition of melt produced near solidus in the phlogopite+ enstatite system

The compositions of melts produced by partial melting near solidus in the phlogopite+enstatite system are necessary to understand the generation of ultrapotassic magmas. We can estimate compositions of the melts produced near solidus in phlogopite +enstatite system by analyzing the quench phlogopite which was the former liquid. All of Mg, Al and Si should be accommodated in the quench crystal of phlogopite, because no other quench crystals than phlogopite was observed in the run products. However, some excess potassium and water may not be accommodated in quench crystals of phlogopite

Average chemical compositions at each pressure of quench crystals of phlogopite are shown in Table 4, and are plotted on a MgO-SiO_2-Al_2O_3 diagram as shown in Fig. 6. The compositions of melts produced at 4 - 8 GPa [12] are more enriched in MgO, or more basic than those at 1 GPa, suggesting that the compositions of melt is enriched in MgO component up to 6 GPa. In the pressure range of 6- 8 GPa, the melt composition becomes less aluminious according to pyrope fractionation.

4. Discussion

4.1. Stability of phlogopite In the mantle

The phase relations of the phlogopite+enstatite system are applicable to assess the stability of phlogopite in the mantle, because the mineral assemblage on solidus of the phlogopite +enstatite system contains three major mantle minerals, forsterite, enstatite and garnet at pressures of 4 - 7 GPa. As addition of other component such as FeO reduce the stability of phlogopite, however, the stability of phlogopite determined in the present study should be regarded as 'maximum phlogopite stability'.

As phlogopite occurrence was reported in the mantle xenoliths from various tectonic settings, i.e., subcontinental lithosphere [3], the mantle beneath the back-arc region [4], and the oceanic mantle beneath oceanic island [7], phlogopite is ubiquitously present in the mantle down to at least 200 km depth. The phlogopite in the mantle is mostly caused by a secondary formation process in which hydrous metasomatic agents scavenging potassium react with peridotites (e.g.,[3,7]). In order to understand the process of formation of secondary phlogopite, the phlogopite stability in the mantles beneath various tectonic settings has to be clarified.

The phlogopite was shown to be stable in lherzolite up to about 6 GPa or 180 km depth by previous studies [1, 11]. Based on the present experimental results, we here discuss the stability of phlogopite in phlogopite-pyroxenites in the wedge mantle being dragged by a down going slab, and garnet harzburgite in the subcratonic mantle. Phlogopite is expected to be more stable in these rocks than in lherzolite, because the geotherms for these regions are lower than that for oceanic mantle and these rocks may not have so large amount of Ca-rich pyroxene as all of the coexisting phlogopite is converted into K-amphibole according to the reaction (1).

Concerning the phlogopite pyroxenites, Sekine and Wyllie [17,18] advocated that the discrete masses of phlogopite-orthopyroxenite or garnet-phlogopite-websterite are formed in the mantle just overlying subducting slabs by hybridization of cool hydrous magma from down going slabs into hotter overlying harzburgite or lherzolite, respectively. These phlogopite-bearing rocks are candidates to transport water and potassium into the deep mantle along with the subducting slab. In phlogopite-orthopyroxenite under the thermal conditions of the normal subducting slab [22], phlogopite would begin to break down gradually and to produce garnet and fluid at about 5 GPa or 150 km depth. However, phlogopite could survive to at least 240 km depth, so that the present experimental results

indicate that H_2O and K_2O could be transported to 240 km depth by phlogopite. In the garnet-phlogopite-websterite, phlogopite reacts with Ca-rich pyroxene according to the reaction (1) at 6GPa or 180 km depth. However, if the amount of phlogopite is so large that phlogopite cannot be consumed by the reaction (1), the remained phlogopite could survive to the depth as in the phlogopite orthopyroxenite. Thus, both the rocks can be transporters of H_2O and K_2O and potential source rocks of potassic magma in the deep mantle as well. Actually the phlogopite-orthopyroxenite in paleo subduction zones is regarded as a source rock of phlogopite-lamproite which erupted in continental margins[23].

Phlogopite is often found in diamond-bearing harzburgite which is considered to constitute near the base of subcratonic lithosphere of 150 - 200 km depths [7,24,25]. This is consistent with the present experimental results as following. The stability of phlogopite in harzburgite constituting the subcratonic mantle is defined by the intersection of the solidus of the phlogopite +enstatite system and subcratonic geotherms (Fig. 7). For a typical geotherm for surface heat flow of 40 mWm^{-2}[26], the stability limit of phlogopite is 7 GPa or 210 km (point A in Fig. 7). However, it should be noted that the stability of phlogopite is limited to a shallower depth for a higher temperature distribution; e.g., 180 km depth for that of 44 mWm^{-2} surface heat flow (point B in Fig. 7).

4.2. Exsolution of garnet and production of fluid

Present study demonstrates that pyrope is present in both the subsolidus and hypersolidus conditions at pressures above 5 GPa. The reaction to form pyrope is not univariant: the amount of pyrope exsolved in the phlogopite and phlogopite + enstatite systems under subsolidus conditions increases with increases in both pressure and temperature. Dehydration proceeds with the exsolution of pyrope as the following schematic reaction;

Starting phlogopite=Al_2O_3-deficient phlogopite + pyrope + K_2O +fluid (H_2O) (2)

Occurrence of the dehydration was confirmed by observation of water drops in the sample charges. Part of expelled potassium from phlogopite should be dissolved in the fluid phase (H_2O) because H_2O fluid leaches K_2O component together with SiO_2 and Al_2O_3 [27,28], and the remainder of potassium would be in the grain boundary. The concentration of potassium along grain boundary was confirmed in a run of phlogopite+enatatite system (6GPa, 1300˚C and 10 hours). Increases in pressure and temperature proceed the reaction (2) to the right hand side; e.g., increase in the amounts of pyrope and released H_2O fluid phase.

4.3. Secondary formation of phlogopite in the continental lithosphere

Replacement of garnet to phlogopite has been petrographically observed in the metasomatized mantle xenoliths, which suggests phlogopite in peridotites from continental lithosphere are formed secondarily (e.g., [3,7]). The metasomatizing agents rise adiabatically from underlying asthenosphere (Fig. 8b) and therefore should be enriched in potassium during upwelling through the undepleted asthenosphere. These agents are inferred to be hydrous silicate melt in high-temperature conditions or a fluid in low temperature conditions. The present study reveals that phlogopite melts incongruently into garnet and hydrous silicate melt and partially break down to garnet and fluid containing K_2O under subsolidus conditions. Thus the metasomatic agents may react with garnet in garnet peridotites and then the secondary phlogopite is formed when they encounter the solidus of the phlogopite+enstatite system. As shown in Figs. 7a and b, the solidus and the typical geotherms for the continental mantle represented by the surface heat flows of 40 and 44 mWm^{-2} cross at about 6 GPa or around 190 km depth, which corresponds to the base of subcratonic lithosphere. However, it should be noted that the negative slope ($dT/dP<0$) of the solidus curve indicates deeper formation of secondary phlogopite for the lower geotherms (Figs. 8a and b).

Stability of phlogopite is sensitive to change of the thermal state of continental lithosphere. For example, if a thermal gradient increases from the surface heat flow of 40 mWm^{-2} to 44 mWm^{-2}, then phlogopite in the region of 170 - 200 km depths are melted out, as depicted by an area marked with a crossed pattern in Fig. 8c. As schematically illustrated in Fig. 8d, when temperature of a certain depth rise from T_A to T_B, the following processes proceed: (1) at temperatures from T_A to T_B, phlogopite decomposes gradually into garnet+ Al-depleted phlogopite+fluid to release fluid,

without melting and (2) at temperature T_B, on the other hand, phlogopite begin to melt out.

These released fluid and silicate melt could serve as new metasomatic agents in the mantle: Released fluid reduce the solidus temperature of a metasomatized peridotites to cause alkaline and hydrous magmas (e.g., kimberlite or lamproite magmatism); Released hydrous silicate melts make secondary enrichment to form phlogopite and other minerals for the sources of alkaline magmas in the shallower part of the mantle.

4.4. Implication to lamproite petrogenesis

Lamproites are ultrapotassic rocks and some of them (olivine lamproite and leucite lamproite) have diamonds [29]. It is inferred from their potassium rich composition that phlogopite should have been in their source material [8].

Recently, K. Sato [30] has revealed that (1) the olivine lamproite with 6 wt% H_2O is saturated with olivine, orthopyroxene and garnet at 5.3 GPa and 1370˚C, and that (2) the magma with 12 wt% H_2O is saturated with orthopyroxene and garnet at 5.7 GPa and 1340˚C. As these conditions are higher than the solidus of the phlogopite+enstatite system determined in the present study, phlogopite in the sources should have been consumed during the partial melting process before magma segregation. Thus, either phlogopite-bearing garnet harzburgite or phlogopite-bearing garnet orthopyroxenite can be the source of olivine lamproite. The problem which rock is the source of the olivine lamproite can be solved by a comparison of melt composition produced near solidi of two rocks with that of the olivine lamproite.

As seen in Fig. 6, the composition of melts produced just above the boundary curve of phlogopite-out in phlogopite-enstatite system at pressures from 5 to 8 GPa, under which conditions the system represents phlogopite-garnet-orthopyroxenite, are different from that of olivine lamproite (point A). On the other hand, the composition of melt produced near solidus from phlogopite harzburgite at pressures from 5 to 8 GPa has not been reported. However, Inoue [31] determined that the Mg/Si ratio of the initial melt produced by a partial melting of hydrous harzburgite up to 15 GPa. His results approximately indicate the melt composition produced by partial melting of phlogopite harzburgite, because phlogopite in the olivine lamproite source is not residual phase. The Mg/Si ratio in partial melt of hydrous harzburgite under 5-6 GPa is in agreement with that of the olivine lamproites [29]. Therefore, the olivine lamproite magma is produced by partial melting of phlogopite-bearing garnet harzburgite, but not by that of phlogopite-garnet-orthopyroxenite.

5. Conclusions

Melting and subsolidus phase relations in the systems of a natural phlogopite and the phlogopite+enstatite were investigated using the uniaxial split-sphere apparatus in the pressure range of 4 - 8 GPa and in the temperature range of 1200 - 1500˚C. Pyrope garnet forms in subsolidus and hypersolidus conditions above 5 GPa in both the systems. Fluid phase gradually forms under subsolidus conditions, and the amount of fluid increase with elevating pressure and temperature in both systems. Solidus temperatures of both the systems have maxima at about 5 GPa and reach negative dP/dT slopes above the pressure. Phlogopite can be stable down to 180-210 km depth in subcalcic garnet harzburgite which constitute the subcratonic lithosphere mantle. Phlogopites could be produced by the interaction between upwelling metasomatic agents and garnet in the host garnet harzburgite near the base of continental lithosphere. If once secondary phlogopite has been formed in the lower part of the subcontinental lithosphere, a metasomatic agent of fluid or hydrous silicate melt could be produced by decomposition of phlogopite on athermal event which raises temperature. These metasomatic agents would induce volcanism or metasomatized peridotites in the shallower parts of the subcontinental lithosphere.

References

[1] Sudo, A. and Tatsumi, Y., Phlogopite and K-amphibole in the upper mantle: Implication for magma genesis in the subduction zones. *Geophy. Res. Lett.*, **17**, 29-32, 1990.

[2] Bailey, D.K., 1982, Mantle metasomatism - continuing chemical change within the Earth. *Nature*, **296**, 525-530.

[3] Menzies, M.A. and Hawkesworth, C.J., MANTLE METASOMATISM, 472pp.,Academic Press, London, 1986.

[4] Arima, M. and Edgar, A.D., A high pressure experimental study on a magnesian-rich leucite-lamproite from the West Kimberley area, Australia: Petrogenesis implication. *Contrib. Mineral. Petrol.*, **84**, 228-234, 1983.
[5] Foley, S.F., An experimental study of olivine lamproite: First results from the diamond stability field, *Geochim. Cosmochim. Acta*, **57**, 483-489, 1993.
[6] Arai, S., K/Na variation in phlogopite and amphibole of upper mantle peridotites due to fractionation of the metasomatism fluids. *Jour. Geology*, **94**, 436-444, 1986.
[7] Nixon, P.H., van Calsteren, P.W.C., Boyd, F.R. and C.J. Hawkesworth, Harzburgite with garnets of diamond facies from southern Africa kimberlites, in "Mantle Xenolith", P.H. Nixon, ed., pp.523-533, John Wiley & Sons, New York, 1987.
[8] Sen, G., Xenoliths associated with the Hawaiian hot spot, in: MANTLE XENOLITH, P.H. Nixon, ed., pp. 359-375, John Wiley & Sons Ltd, New York, 1987.
[9] Kushiro, I., Syono, Y. and Akimoto, S., Stability of phlogopite and possible presence of phlogopite in the Earth's upper mantle. *Earth. Planet. Sci.Lett.*, **3**, 197-203, 1967.
[10] Yoder, H.S. Jr. and Kushiro, I., Melting of a hydrous phase: phlogopite. *Am.Jour.Sci.*, **267A**, 558-582, 1969.
[11] Modreski, P.J. and Boettcher, A.L., The stability of phlogopite + enstatite at high pressures: A model for micas in the interior of the Earth. *Am. Jour. Sci.*, **272**, 852-869, 1972.
[12] Modreski, P.J. and Boettcher, A.L., Phase relationships of phlogopite in the system K_2O-MgO-CaO-Al_2O_3-SiO_2-H_2O to 35 kilobars: A better model for micas in the interior of the Earth. *Am. Jour. Sci.*, **272**, 385-414, 1973.
[13] Wendlant, R.F. and Eggler, D.H., The origins of potassic magmas: stability of phlogopite in natural spinel lherzolite and in the system $KAlSiO_4$-MgO-SiO_2-H_2O-CO_2 at high pressures and high temperatures. *Am.Jour.Sci.*, **280**, 421-458, 1980.
[14] Foley, F.S., Wayne, R.T. and Green, D.H., The effect of fluorine on the phase relationships in the system $KAlSiO_4$-Mg_2SiO_4-SiO_2 at 28 kbar and solution mechanism of fluorine in silicate melts, *Contrib. Mineral. Petrol.*, **93**, 46-55, 1986.
[15] Tronnes, R.G., Takahashi,E. and Scarfe,C.M., 1986, Stability of K-richterite and phlogopite to 14GPa. *EOS* **69**, 1510-1511.
[16] Luth, R.W., Tronnes, R.G., Canil, D., Volatile phases in the Earth's mantle. In Luth,R.W. (ed.), Experiments at High Pressure and Applications to the Earth's Mantle. Mineral. Assoc. Canada Short Course Handbook 21, pp.445-485.1993.
[17] Sekine, T. and Wyllie, P.J., Phase relationships in the system $KAlSiO_4$-Mg_2SiO_4-SiO_2-H_2O as a model for hybridization between hydrous siliceous melts and peridotite. 1982, *Contrib. Mineral. Petrol.*, **79**, 368-374, 1982.
[18] Sekine, T. and Wyllie, P., Synthetic systems for modeling hybridization between hydrous siliceous magmas and peridotite in subduction zones, *Journal of Geology*, **90**, 734-741, 1982.
[19] Ito, E. and Yamada, H., Stability relations of silicate spinels, ilmenite and perovskite, in: High-pressure Research in Geophysics, Akimoto,S. and Manghnani,M.N., ed., pp. 405-419, Reidel, Dordrecht, 1982.
[20] Yagi, T., Akaogi, M., Shimomura, O., Suzuki, T. and Akimoto, S., In site observation of olivine-spinel phase transformation in Fe_2SiO_4 using synchrotoron radiator. *J.Geophys.Res.*, **92**, 6207-6213, 1987.
[2l] Akimoto,S., and Sato, Y., High-pressure transformation in Co_2SiO_4 olivine and some geophysical implications, *Physics of Earth and Planetary Interiors*, **1**, 498 -504, 1968.
[22] Thompson, A.B., Water in the Earth's upper mantle, *Nature*, **358**, 295-302, 1992.
[23] Mitchell, R.H. and Bergman, S.C., 447 pp., Petrology of lamproites. Plenum Press, New York, 1990.
[24] Nixon, P.H., Kimberlitic xenoliths and their cratonic setting. in "Mantle Xenolith", pp. 215-242, P.H. Nixon, ed., John Wiley and Sons, New York, 1987.
[25] Boyd, F.R., D.G. Pearson, P.H. Nixon and S.A. Mertzman, Low-calcium garnet harzburgites from southern Africa: their relations to craton structure and diamond crystallization, *Contrib. Mineral. Petrol.*, **113**, 352-366, 1993.
[26] Finnerty, A.A. and F.R. Boyd, Thermobarometry for garnet peridotites: basis for the determination of thermal and compositional structure of the upper mantle.n "Mantle Xenolith", P.H. Nixon, ed., pp. 403-412, John Wiley and Sons, New York, 1987.

[27] Nakamura, Y. and Kushiro, I., Composition of the gas phase in Mg_2SiO_4-SiO_2-H_2O at 15kbar. *Carnegie Inst. Washinghton Yearb.*, **73**, 255-258, 1973.
[28] Ryabchikov, I.D. and Boettcher, A.L., Experimental evidence at high pressure for potassic metasomatism in the upper mantle of the earth. *Am.Mineral*., **65**, 915-919, 1980.
[29] Jaques, A.L., Lewis, J.D.,Smith, C.B., The kimberlites and lamproites of Western Australia. *Geol. Surv. Western Aust. Bull.*, **132**, 268 pp., 1986.
[30] Sato, K., A high-pressure experimental study on an olivine lamproite: application to its petrogenesis, in press.
[31] Inoue, T, Effect of water on melting phase relations and melt composition in the system Mg_2SiO_4-$MgSiO_3$-H_2O up to 15 GPa, *Phys. Earth Planet. Inter.*, **85**, 237-263, 1994.
[32] Zhang, J and Herzberg,C., Melting experiment on anhydrous peridotite KLB-1 from 5.0 to 22.5 GPa, *J.Geophys.Res.*, **99**, 17,729 - 17,742, 1994.
[33] Pollack H.N. and Chapman D. S., On the regional variation of heatflow, geotherms and lithospheric thickness. *Tectonophysics* **38**, 279-296.

Table 1. Starting composition of phlogopite and the ideal phlogopite for comparison.

wt%	This study		Ideal phlogopite
	(n=7)	1-s	
SiO2	40.01	0.37	43.2
TiO2	0.40	0.03	
Al2O3	14.87	0.30	12.21
FeO	1.83	0.03	
MnO	0.07	0.04	
MgO	25.04	0.28	28.99
Na2O	0.32	0.03	
K2O	11.27	0.09	11.29
H2O			4.31
total	93.81		100
	O=22		
Si	5.741		6
Ti	0.0433		
Al	2.5153		2
Fe	0.2198		
Mn	0.0082		
Mg	5.3554		6
Na	0.0878		
K	2.0623		2
total	16.0332		16

Table 2. Summary of conditions of experiments.

P, GPa	T, ℃	Duration, (min)	Run products
phlogopite			
4	1200	120	Ph
4	1300	60	Ph
4	1350	30	Ph
4	1400	30	Fo, q-Xl
5	1200	60	Ph, Py
5	1300	60	Ph, Py
5	1350	30	Ph, Py
5	1400	30	Fo, Py, Sp, q-Xl
6	1300	60	Ph, Py
6	1350	30	Ph, Py
6	1400	30	Py, q-Xl
6	1500	30	Fo, Py, q-Xl
8	1250	120	Ph, Py, Fo, q-Xl
8	1300	60	Ph, Py, Fo, q-Xl
8	1350	90	Py, Fo, q-Xl
8	1400	30	Py, En, q-Ph
phlogopite + enstatite			
4	1200	120	Ph, En
4	1300	60	Ph, En
4	1350	30	Ph, En, Fo, q-Xl
4	1400	30	En, Fo, q-Xl
5	1200	60	Ph, En, Py
5	1300	60	Ph, En, Py, Fo
5	1350	30	En, Py, Fo, ±q-Xl
5	1400	30	En, Py, Fo, q-Xl
6	1300	60	Ph, En, Py
6	1300	600	Ph,En,Py
6	1350	30	Ph, En, Fo, ±q-Xl
6	1400	30	En, Py, q-Xl
8	1250	120	En, Py, Ph
8	1300	60	En, Py, Ph, q-Xl
8	1350	90	En, Py, q-Xl
8	1400	30	En, Py, q-Xl

Ph= phlogopite; En= enstatite; Py=ptrope; Fp=forsterite
q-Xl= quench crystal

Table 3. Chemical composition of phlogopite in the phlogopite and the phlogopite+enstatite system

Phlogopite in the phlogopite system

	4G1300C	1-s(n=5)	5G1300C	1-s (n=5)	6G1300C	1-s (n=7)	8G1250C	1-s (n=5)
SiO2	41.04	0.22	40.91	0.78	40.73	0.40	41.69	0.28
TiO2	0.38	0.02	0.34	0.07	0.21	0.02	0.19	0.02
Al2O3	15.17	0.19	15.21	0.66	14.35	0.23	12.93	0.13
FeO	0.15	0.06	0.01	0.02	0.31	0.08	0.05	0.03
MgO	25.47	0.33	25.95	0.51	25.32	0.32	26.69	0.33
Na2O	0.24	0.05	0.22	0.27	0.31	0.05	0.24	0.07
K2O	11.45	0.18	11.33	0.45	11.63	0.45	11.35	0.27
total	93.90	0.65	93.98	1.15	92.87	0.45	93.14	0.99
	O=22							
Si	5.8205		5.7930		5.8595		5.9628	
Al(4)	2.1795		2.207		2.1405		2.0372	
Al(6)	0.3567		0.3325		0.2932		0.1418	
Fe	0.0177		0.0015		0.0368		0.0204	
Mg	5.3839		5.4767		5.4301		5.6906	
Ti	0.0406		0.0364		0.0337		0.0204	
#1	0.2011		0.1529		0.2062		0.1268	
Na	0.0666		0.0598		0.053		0.0667	
K	2.0717		2.0469		2.1356		2.0701	
total	15.94		15.9542		16.0191		15.9958	
Mg+Si	11.2044		11.2697		11.2898		11.6534	
Al+AL	5.0724		5.079		4.8674		4.358	
Mg+2Al	10.4563		10.5557		10.2975		10.0486	
2Si+V	11.8421		11.7389		11.9252		12.0524	

Phlogopite in the phlogopite+enstatite system

	4G1300C	1-s(n=5)	5G1300	1-s(n=3)	6G1300(1h)	1-s(n=4)	6G1300(10h)	1-s(n=4)	8G1250	1-s(n=4)
SiO2	41.71	0.65	41.33	0.57	45.37	0.90	45.95	0.88	44.71	0.57
TiO2	0.32	0.02	0.24	0.04	0.26	0.05	0.11	0.06	0.17	0.01
Al2O3	13.55	0.19	13.19	0.32	8.74	0.40	10.41	0.53	10.56	0.14
FeO	0.02	0.03	0.01	0.01	0.02	0.02	0.02	0.02	0.01	0.00
MgO	26.10	0.48	26.34	0.64	26.73	0.86	26.59	1.12	26.87	0.23
Na2O	0.29	0.10	0.25	0.15	0.11	0.02	0.11	0.06	0.17	0.05
K2O	11.17	0.20	11.31	0.19	11.28	0.56	11.89	0.35	10.91	0.23
total	93.17	1.34	92.67	1.07	93.52	1.39	95.08	1.33	93.40	0.71
	O=22									
Si	5.9513		5.9401		6.3921		6.4053		6.3246	
Al(4)	2.0487		2.0599		1.6079		1.5947		1.6706	
Al(6)	0.2295		0.1751		0.0384		0.1171		0.0886	
Fe	0.0027		0.0006		0.0012		0.0024		0.0008	
Mg	5.5506		5.6418		5.6301		5.5237		5.6658	
Ti	0.0339		0.0258		0.0283		0.0119		0.0176	
#1	0.1833		0.1567		0.2888		0.3449		0.2262	
Na	0.0792		0.0693		0.0294		0.0298		0.0477	
K	2.0326		2.0739		2.0628		2.1138		1.9694	
total	15.9316		15.9882		15.8126		15.7987		15.7862	
Mg+Si	11.5019		11.5819		12.0222		11.929		11.9904	
Al+Al	4.5564		4.47		3.2926		3.4236		3.5204	
Mg+2Al	10.107		10.1118		8.9227		8.9473		9.1862	
2Si+V	12.0859		12.0369		13.073		13.1555		12.8754	

Table 4. Chemical composition of quench phlogopite in phlogopite-enstatite system.

wt%	4G1400℃ (n=6)	1-s	5G1400℃ (n=5)	1-s	6G1400℃ (n=8)	1-s	8G1350℃ (n=3)	1-s
MgO	22.51	5.12	21.02	4.17	24.89	2.261	24.86	1.05
Na2O	0.15	0.08	0.09	0.082	0.14	0.084	0.13	0.11
Al2O3	12.03	1.21	12.23	0.627	9.24	0.697	8.25	0.75
SiO2	50.91	1.32	48.96	4.208	45.61	1.024	48.20	3.45
K2O	9.02	2.81	10.17	1.539	11.66	0.574	12.44	0.59
TiO2	0.32	0.04	0.48	0.076	0.44	0.244	0.38	0.08
FeO	0.01	0.01	0.05	0.052	0.03	0.03	0.04	0.04
total	94.95	2.14	92.97	1.218	92.00	3.29	92.27	3.99

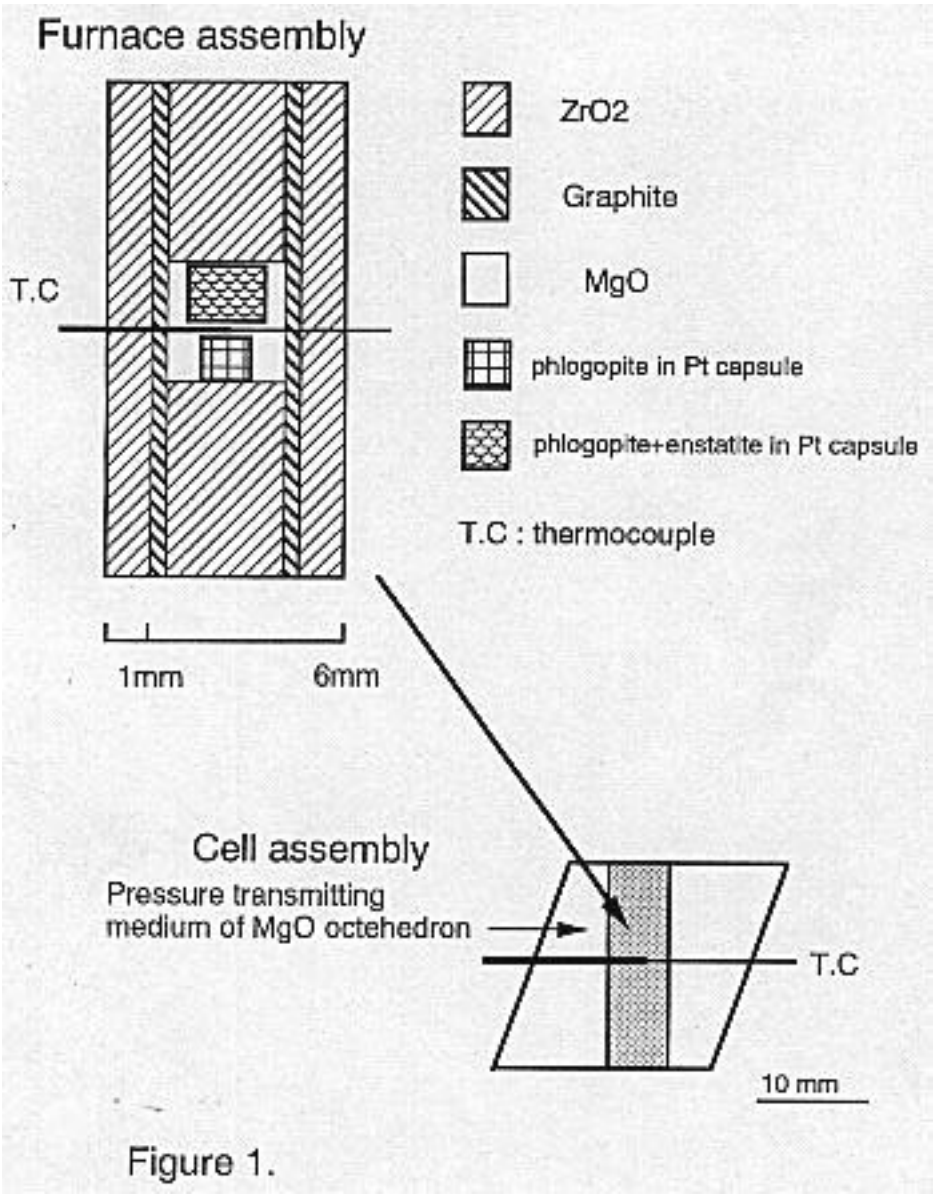

Figure 1. Cross section of the furnace assembly used for high-pressure phase equilibrium experiments. The assembly is inserted into the MgO octahedron pressure medium.

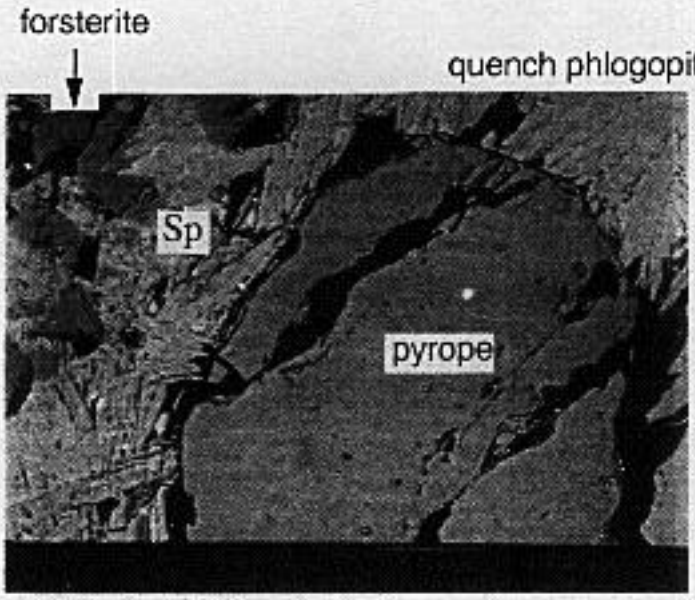

5GPa, 1400 °C

50um

(a)

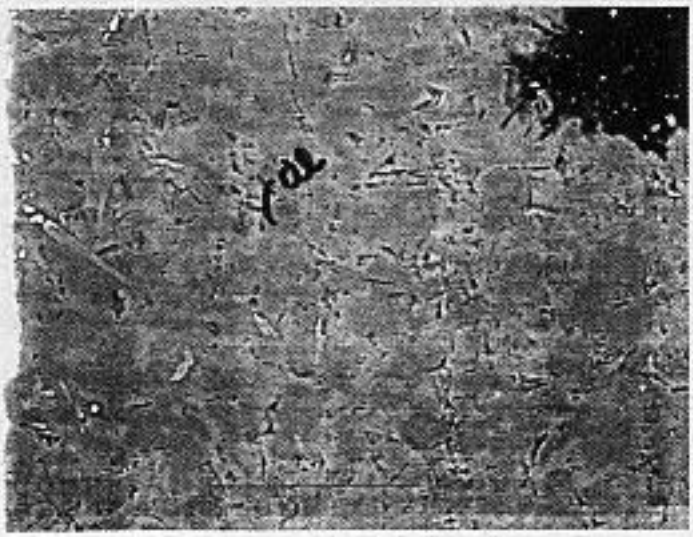

100um

(b) 6GPa, 1350°C

Figure 2

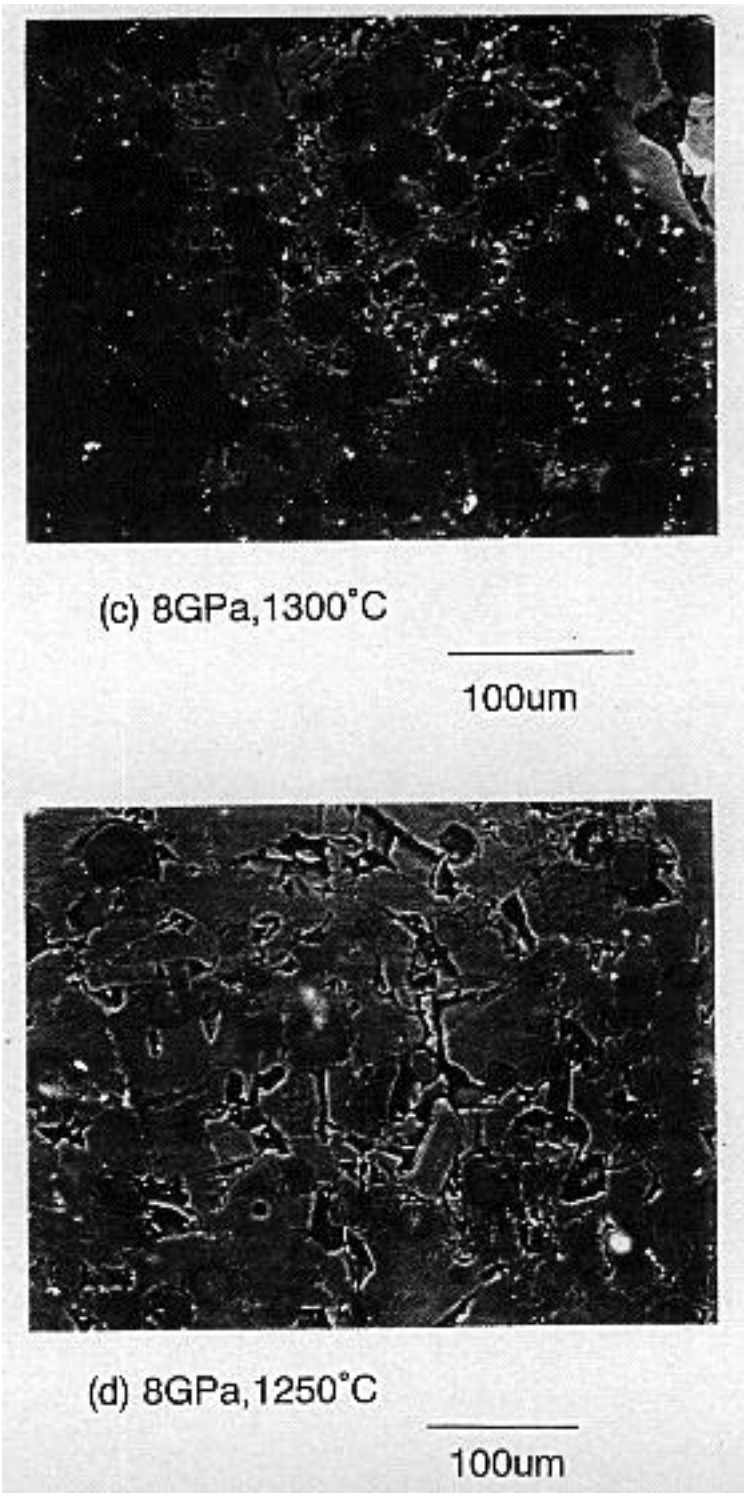
(c) 8GPa,1300°C
100um
(d) 8GPa,1250°C
100um

Figure 2. Back-scattered microphotographs. (a) Run product of the phlogopite system quenched at 5GPa and 1400℃. Pyrope garnet, forsterite, spinel and quenched phlogopite are observed. (b) Run product in the phlogopite+enstatite system quenched at 6GPa and 1350℃. Phenocrystal phlogopite, quenched phlogopites, enstatite and garnet are observed. Coexistence of solid phlogopite and quench phlogopite (the former liquid) is evidence for occurrence of the interval melting. (c) Run product quenched at 8GPa and 1300℃ of the natural phlogopite. Solid phlogopite, quenched phlogopite, enstatite and garnet are coexisting. (d) Run product quenched at 8GPa and 1250℃ of the natural phlogopite. Phenocrystal phlogopite, enstatite and garnet are observed. Melting is not observed.

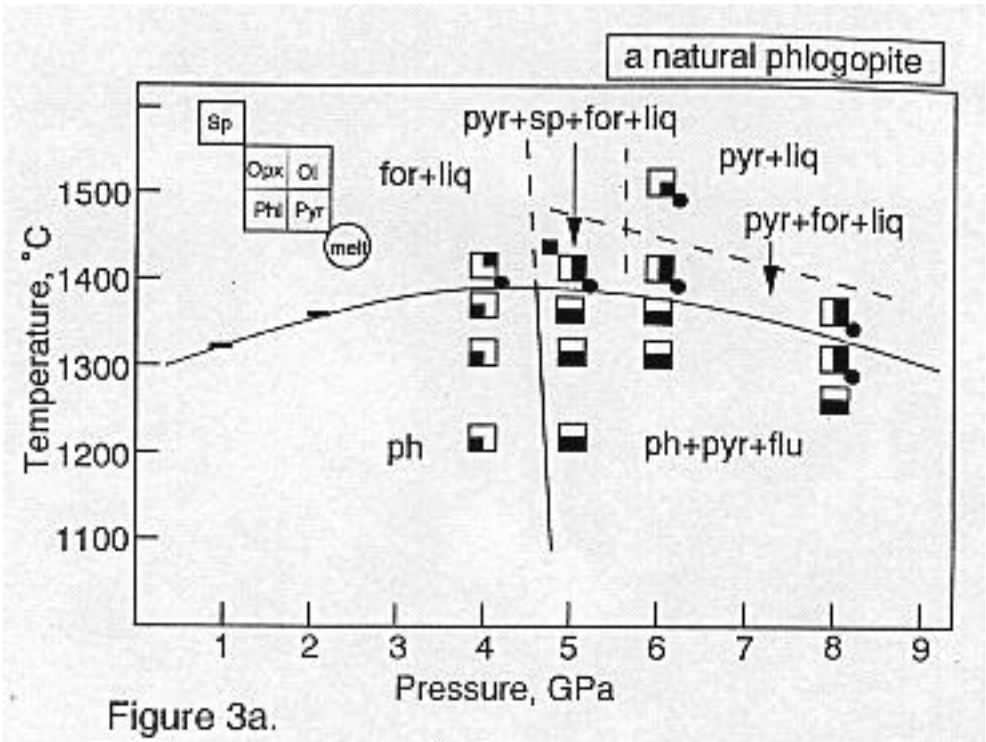

Figure 3a.

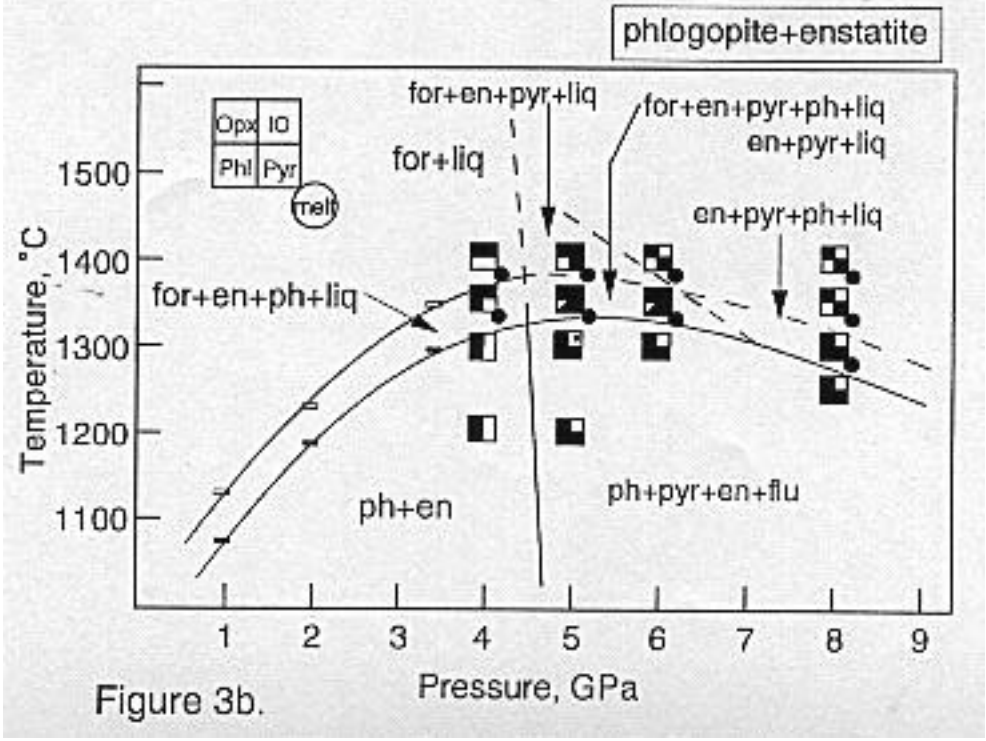

Figure 3b.

Figure 3a. Phase relations in the phlogopite system without additional water. Phases present are shown by solid square in symbols. The boundary for pyrope garnet occurrence is not univariant curve. The data of the lower pressure conditions with rectangle are from Yoder and Kushiro (1969) and Modreski and Boettcher (1972).
Figure 3b. Phase relations in the phlogopite+enstatite system without additional water. The upper curve with dashed line indicates the solidus. The upper curve indicates the disappearance of phlogopite. The data of the lower pressure conditions are from Modreski and Boettcher (1972) [10].

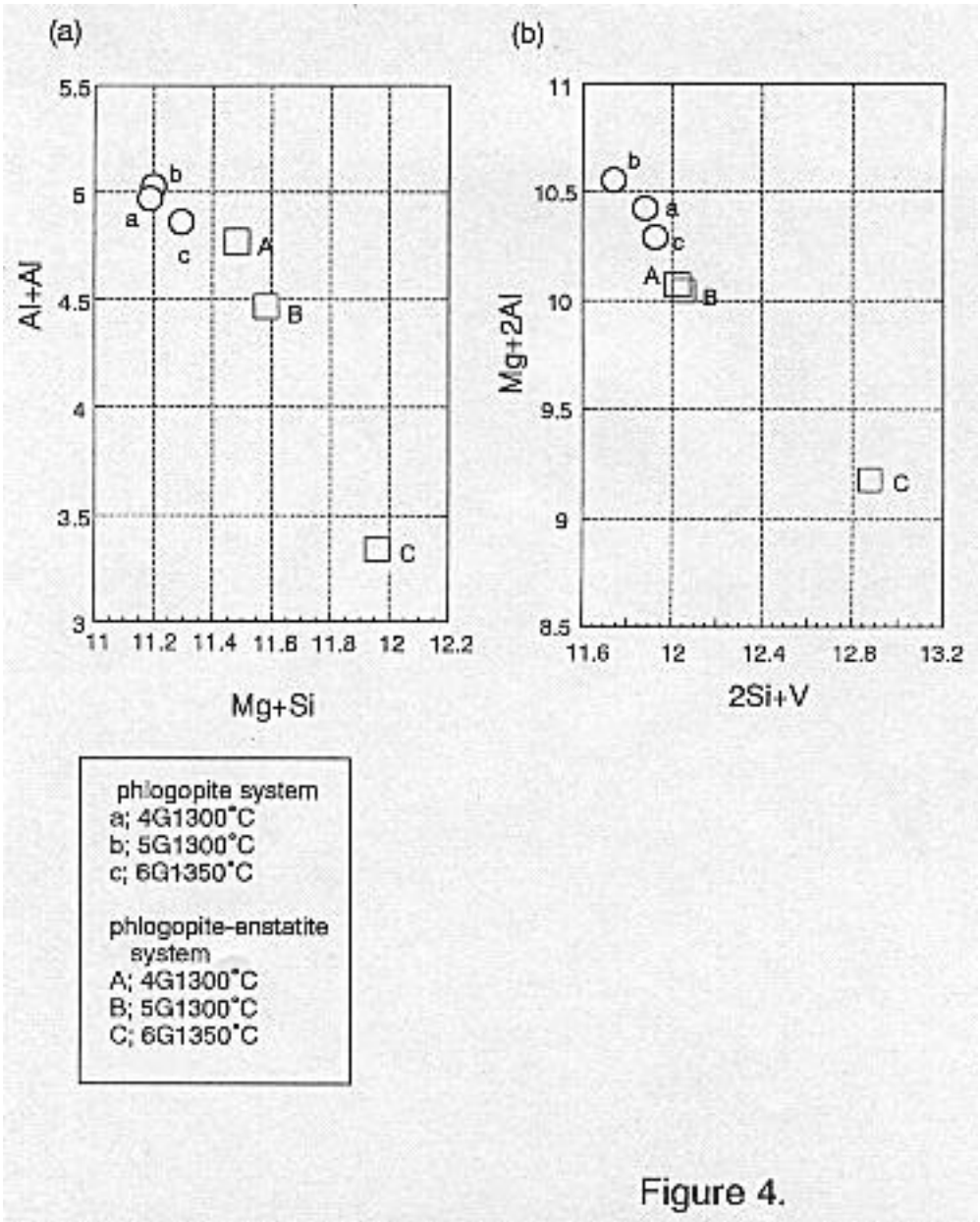

Figure 4.

Figure 4. The correlations between Mg+2Al and V(vacancy)+2Si and between Al+Al and Mg+Si in the phlogopites produced in systems; phlogopite and enstatite+phlogopite.

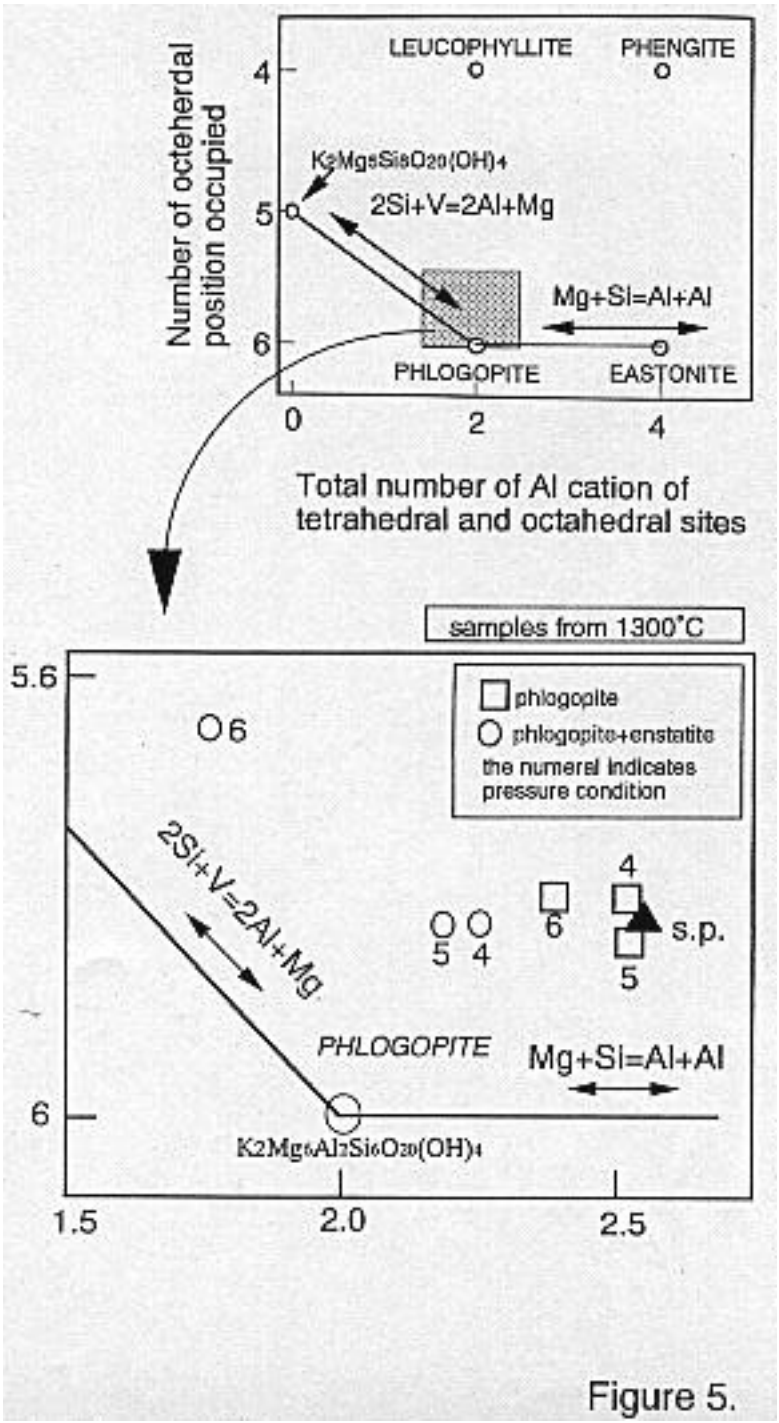

Figure 5. Compositional change of phlogopite due to cation substitutions of 2Si+V=2Al+Mg and Mg+Si=Al+Al at 1300°C. Numbers attached to the plotted points denote pressure (GPa). V: vancancy.

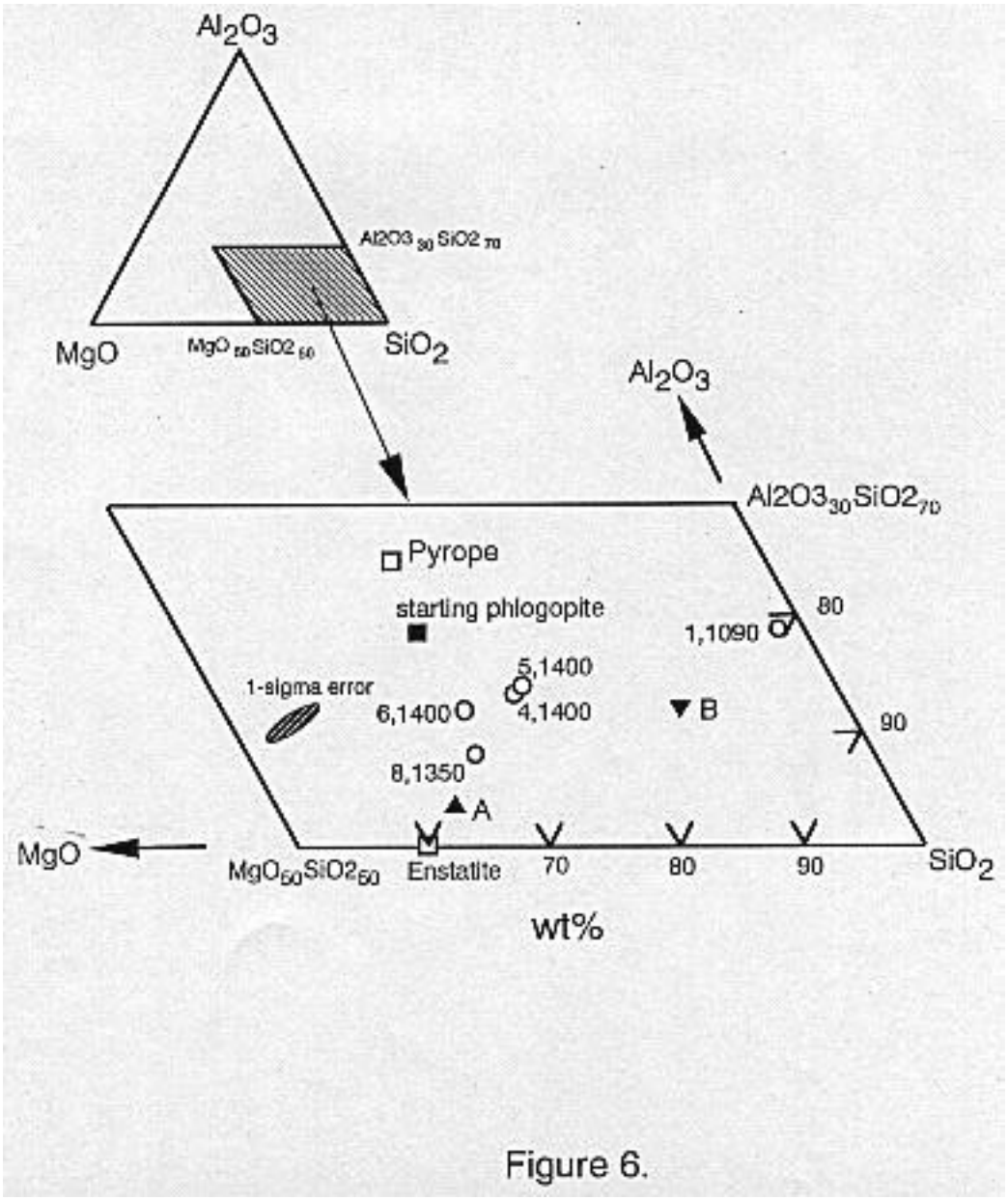

Figure 6.

Figure 6. Compositions of the melt that is formed by small degree of partial-melting in the enstatite + phlogopite system, plotted on the plane MgO-Al_2O_3-SiO_2. The numbers attached to the plotted points indicate experimental pressure in GPa (left) and temperature (°C) (right). The data of 1GPa is from Modreski and Boettcher [11]. Solid triangles A and B indicate plotted of composition of olivine lamproite and leusite lamproite, respectively. One standard deviation of analyzed chemical composition of is represented by the ellipse.

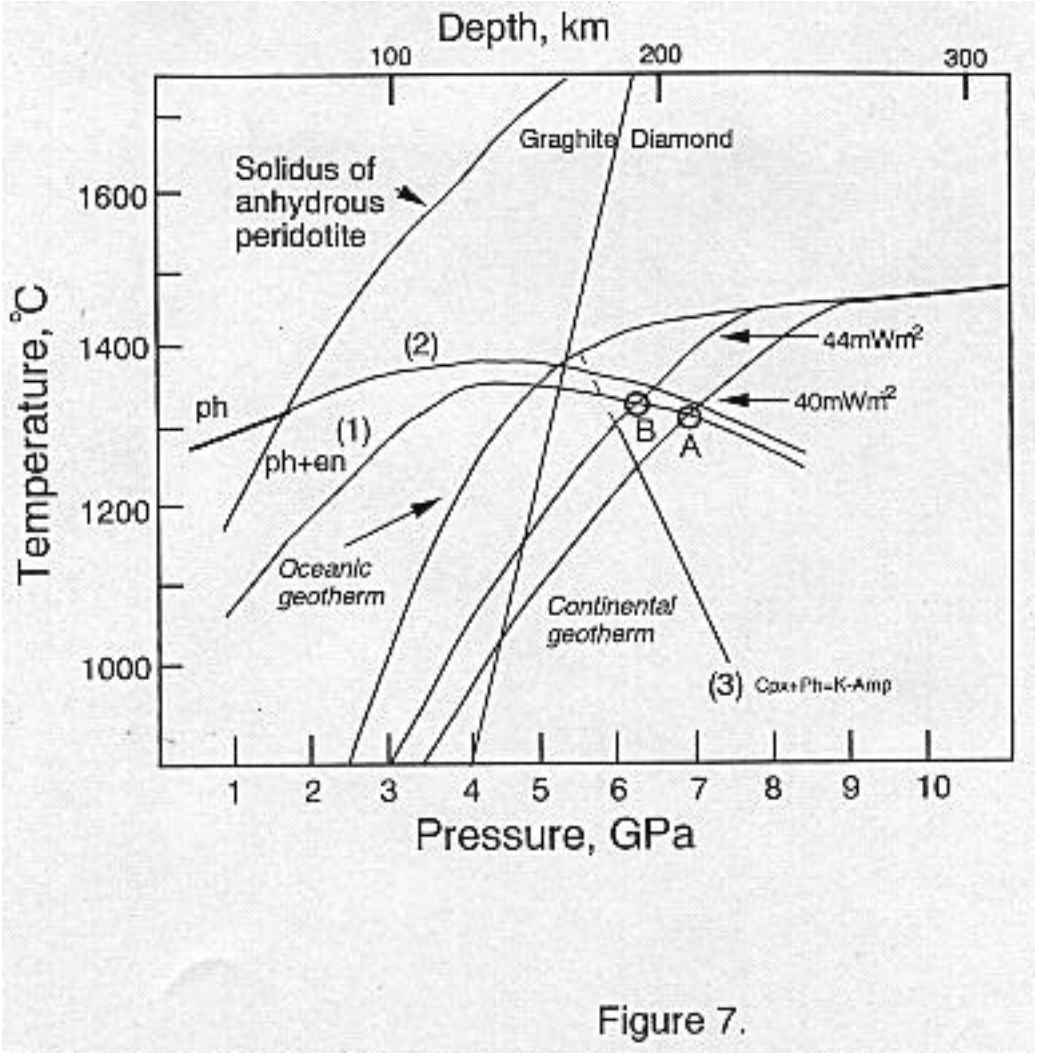

Figure 7.

Figure 7. Pressure-temperature projection of reactions related to the stability of phlogopite and the geotherms for oceanic mantle and stable continental mantle. The anhydrous solidus of a peridotite is from Zhang and Herzberg (1994) [32]. Boundaries; (1): stability limit of phlogopite in the phlogopite+enstatite system (present study and Modreski and Boettcher [10]), (2): stability limit of phlogopite in the phlogopite system (present study and Modreski and Boettcher [10]), and (3):stabilty of phlogopite in lherzolite (Sudo and Tatsumi, 1990) [1]. Point A: stability limit of phlogopite in Cpx-free garnet harzburgite for a geotherm of 40 mWm $^{-2}$ for surface heat flow [33]. Point B: that for with a geotherm of 44 mWm $^{-2}$ [33].

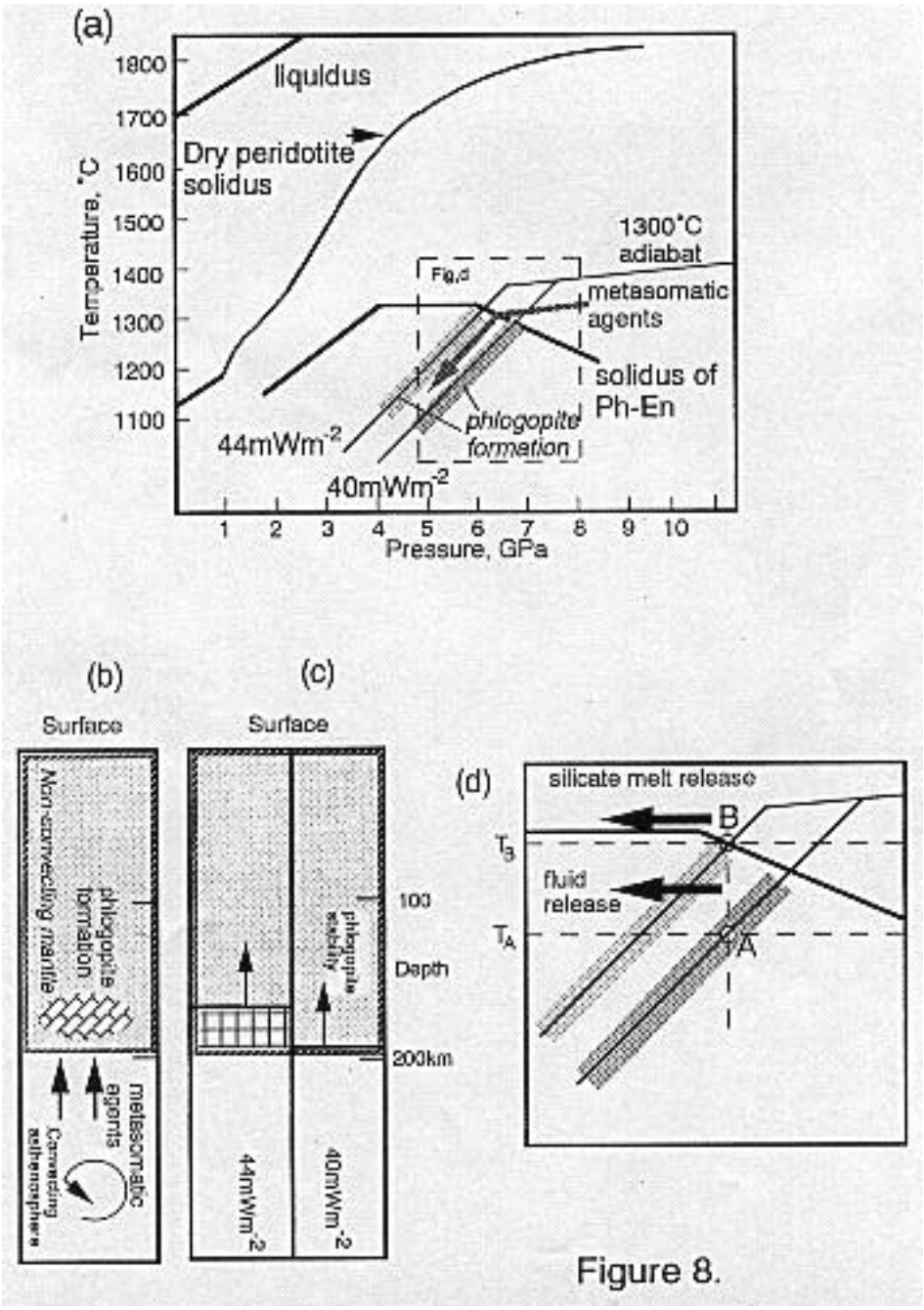

Figure 8.

Figure 8. Potential region for phlogopite formation by infiltration of upwelling metasomatic agents into peridotites at the base of continental lithosphere. (a) possible phlogopite forming region in the continental lithosphere with various geotherms. Extension of potential region for phlogopite formation to more deeper region with the cooler geotherm is shown. (b) Schematic depiction of secondary formation of phlogopite at the base of continental lithosphere by interaction of upwelling metasomatic agents with garnet in clinopyroxene free garnet harzburgite. (c),(d) A swept-away process of phlogopites in the region containing secondary formed phlogopites caused by the temperature increase in the region. In a region with crossroad-pattern in the lower part of the square in Fig.(c), phlogopite gradually decomposes with fluid release at temperature T_A - T_B (point A in Fig.d) and begins to melt at T_B with release of silicate melt (point B).